

Electron microscopy applications – materials science



Investigation of the structure of crystalline materials in the scanning electron microscope using electron backscatter diffraction (EBSD)

Carol Trager-Cowan^{1*}, S. Vespucci¹, G. Naresh-Kumar¹,
D. Maneuski², V. O'Shea², B. M. Jablon¹, A. Vilalta-Clemente³,
A. J. Wilkinson³, K. Mingard⁴ and A. Winkelmann^{1,4}

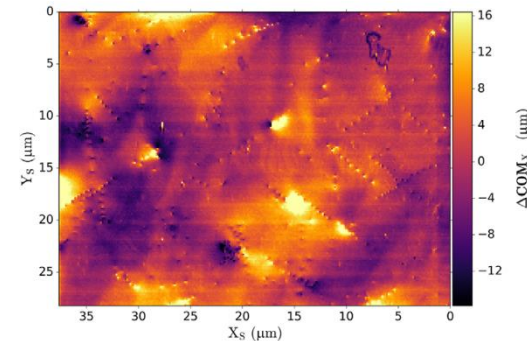
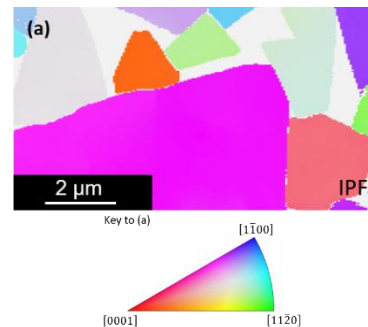
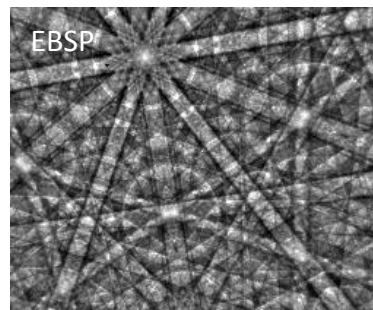
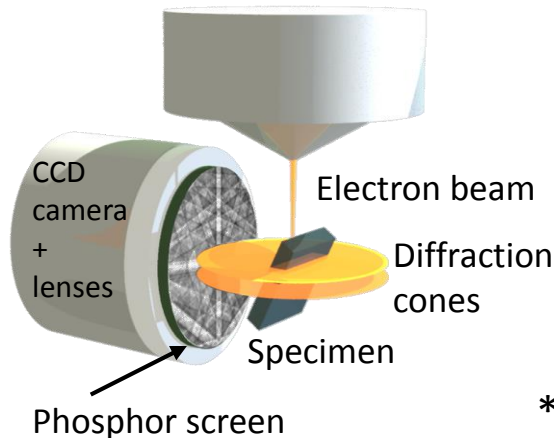
¹Department of Physics, SUPA, University of Strathclyde, Glasgow, UK

²School of Physics and Astronomy, SUPA, University of Glasgow, Glasgow, G12 8QQ, UK

³Department of Materials, University of Oxford, Oxford, UK

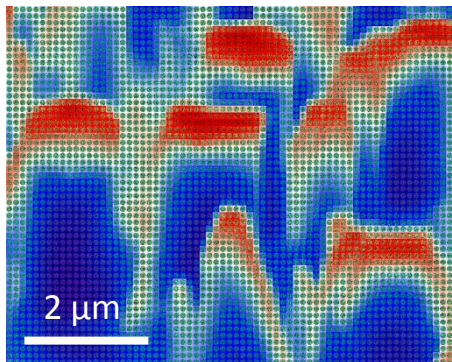
⁴National Physics Laboratory, Teddington, TW11 0LW, UK

⁵Academic Centre for Materials and Nanotechnology,
AGH University of Science and Technology, Krakow, Poland

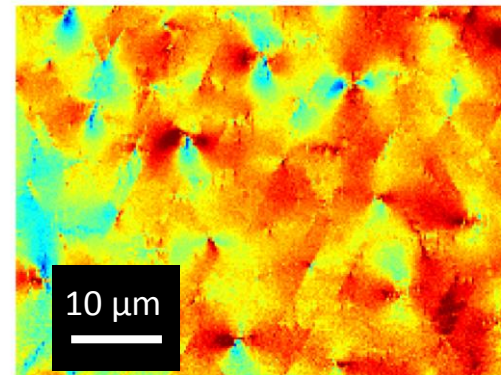


(c) Map of x -deviation of COM from mean

*E-mail: c.trager-cowan@strath.ac.uk



Talk Outline



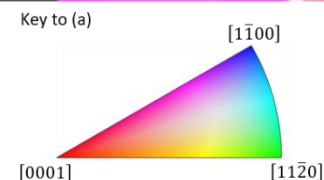
- Description of imaging modes in the scanning electron microscope (SEM), particularly those **exploiting diffraction** and thus capable of imaging defects and strain in crystalline materials, in particular:

- **Electron backscatter diffraction (EBSD)**
- **Some applications of EBSD**

- **Limitation of conventional EBSD systems**

- **Advantages of direct electron detection (using hybrid pixel detectors)**

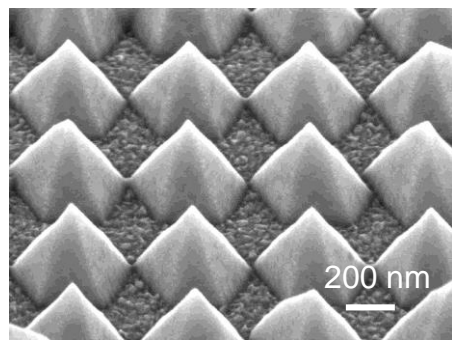
- **Some new applications made possible with direct electron detection**



Imaging Modes in the Scanning Electron Microscope (SEM)

Electron beam
select energy between 0.2 to 30 keV

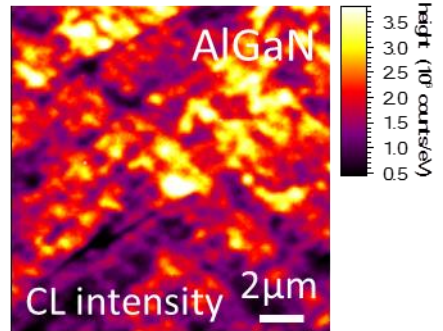
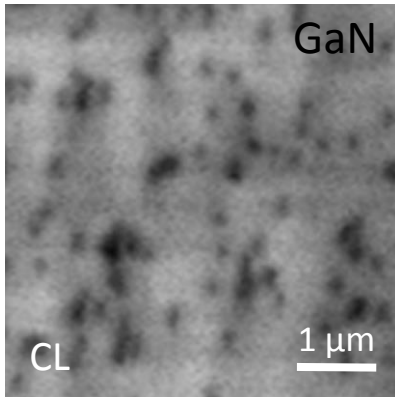
Secondary electrons
- surface imaging, topography



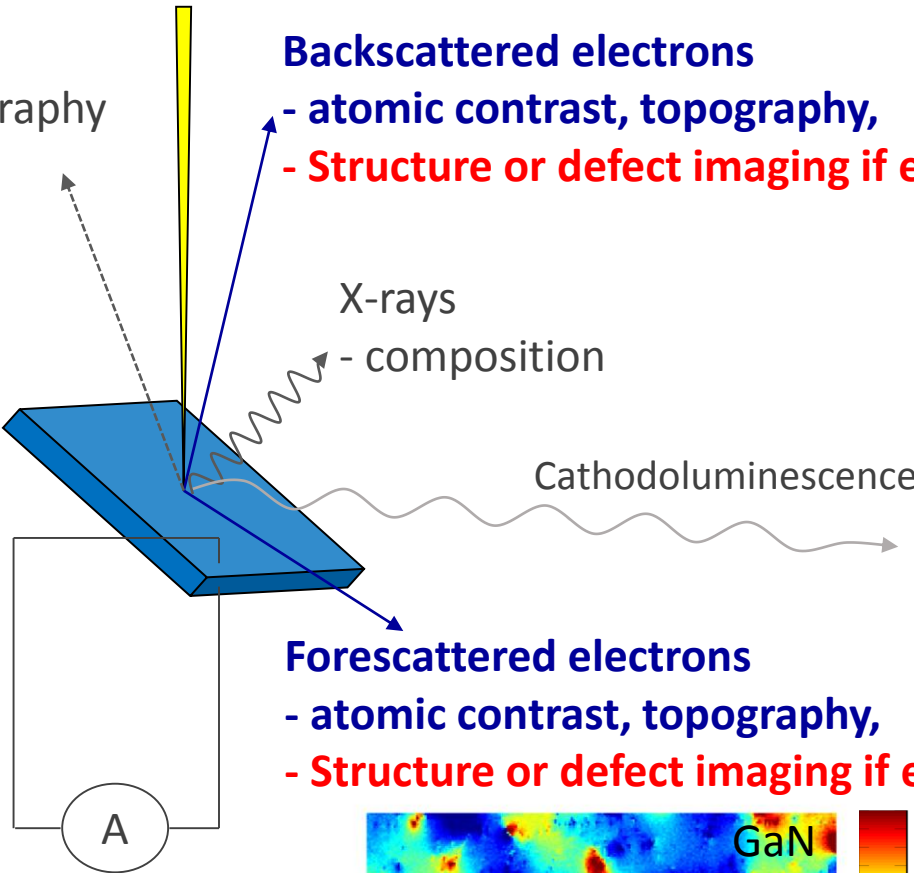
Backscattered electrons
- atomic contrast, topography,
- **Structure or defect imaging if electrons are diffracted**

X-rays
- composition

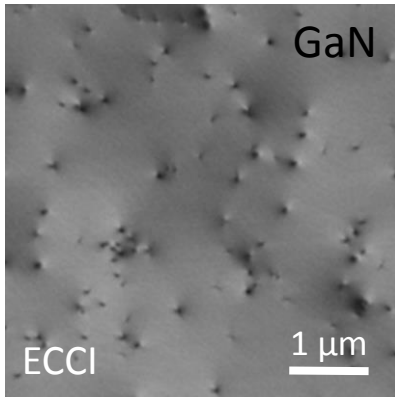
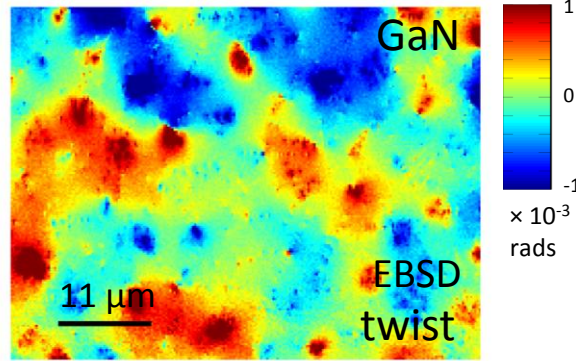
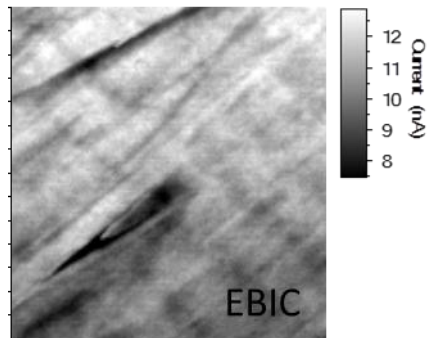
Cathodoluminescence



Foreshattered electrons
- atomic contrast, topography,
- **Structure or defect imaging if electrons are diffracted**



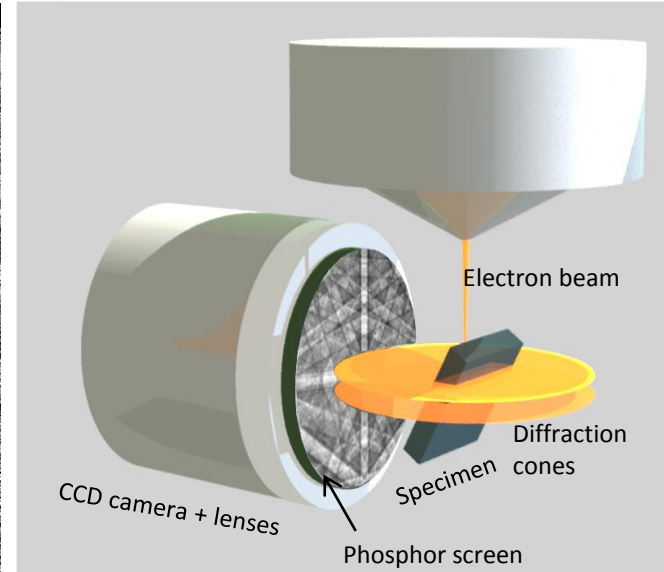
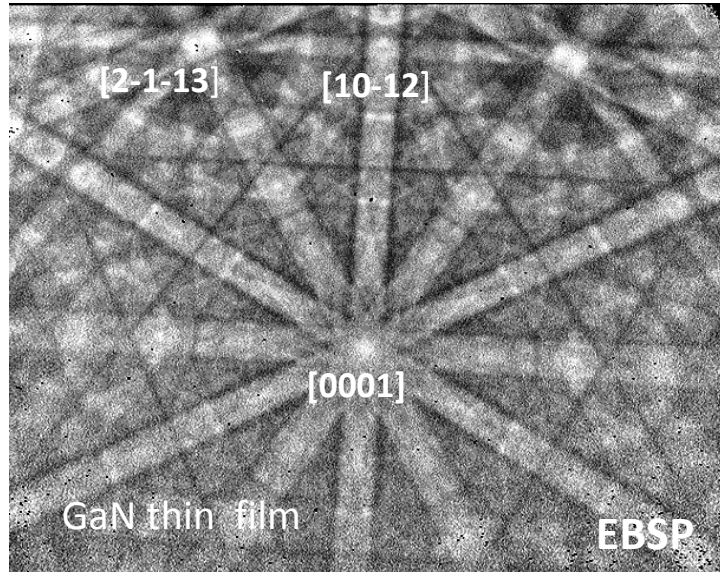
Electron beam induced current



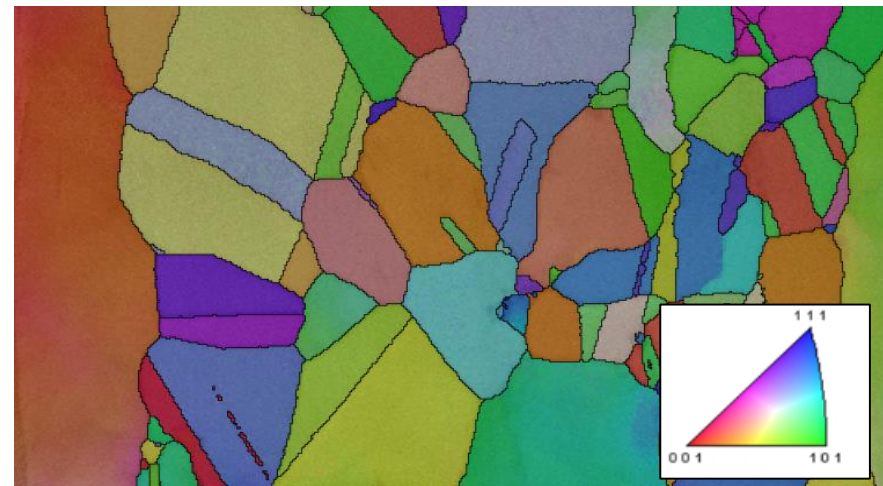
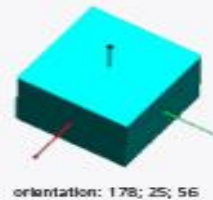
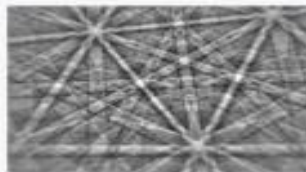
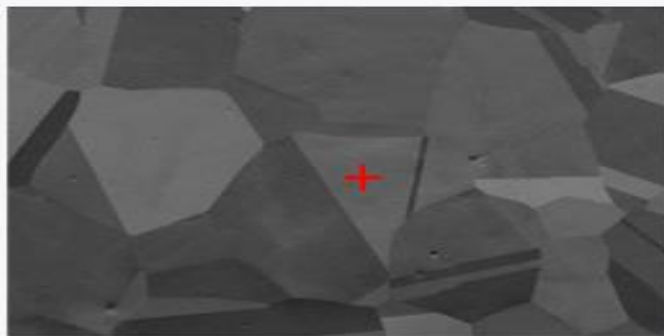
What is Electron Backscatter Diffraction (EBSD)?

EBSD provides information on:

- Crystal structure
- Crystal orientation
- Misorientation
- Grain size
- Grain boundaries
- Strain
- Defects



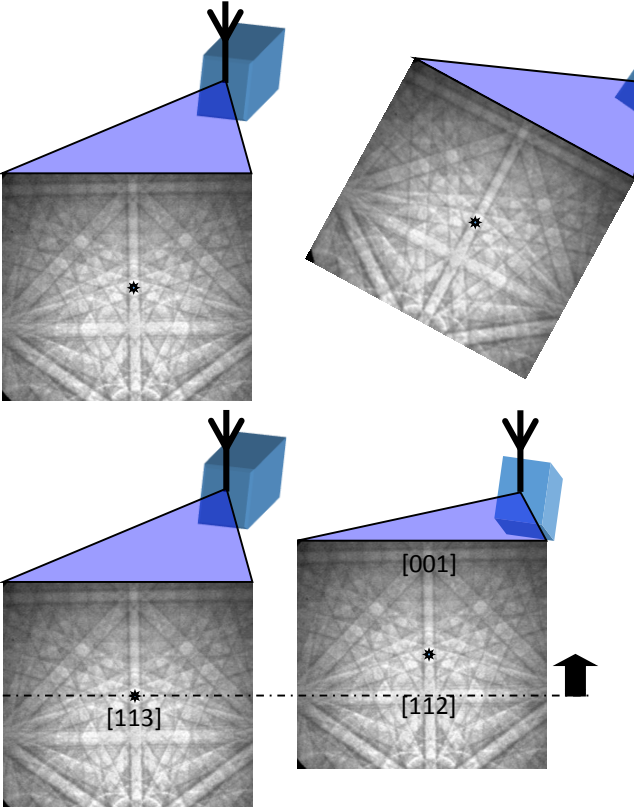
Note the phosphor screen is of order 40 mm × 30 mm in size where the number of pixels can range from 640 × 480 to 1280 × 960 to even 2k × 2k. So an effective pixel size ranges from 60 μm × 60 μm down to 20 μm × 20 μm.



Orientation map of a nickel sample courtesy of Ken Mingard, NPL

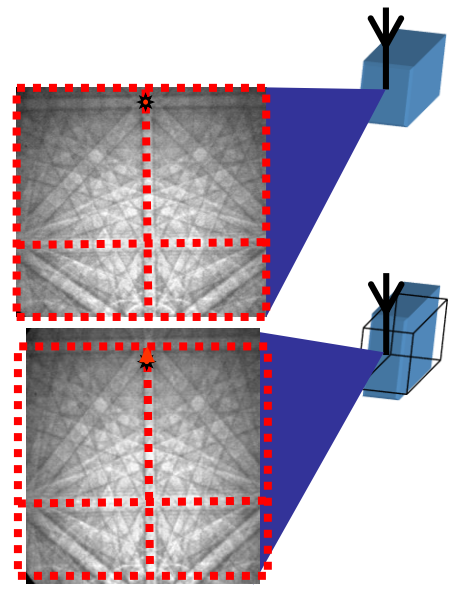
From:
<http://www.ebsd.com/index.php/component/content/article/83-ebsd-for-beginners/125-introduction>

Measuring tilt, rotation & strain with EBSD



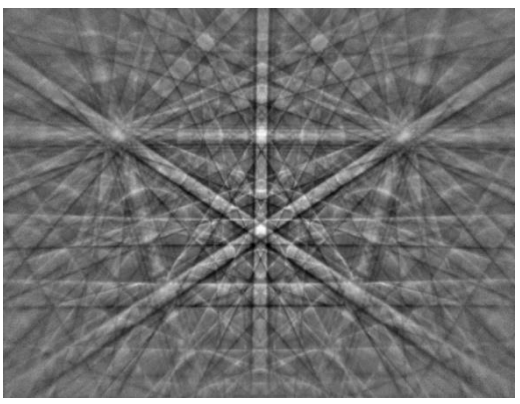
Rotating (or twisting) a crystal rotates its EBSD pattern. This illustration shows a rotation around the * [113] direction (in silicon).

Tilting a crystal shifts its EBSD pattern. This illustration shows a tilt of $\approx 10^\circ$.

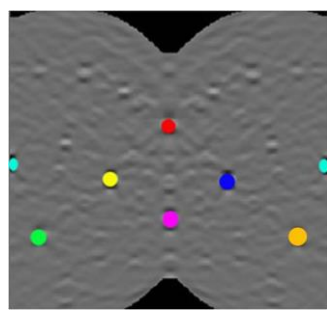


A distortion of a crystal will produce a distortion of the EBSD pattern.

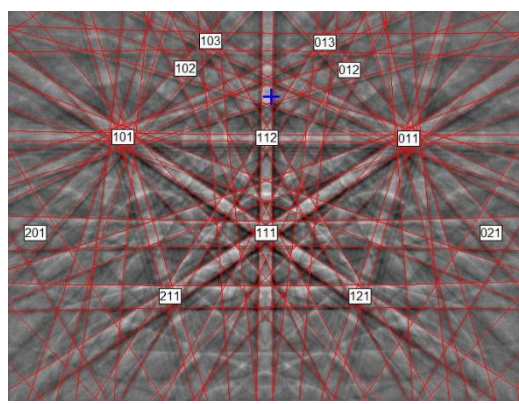
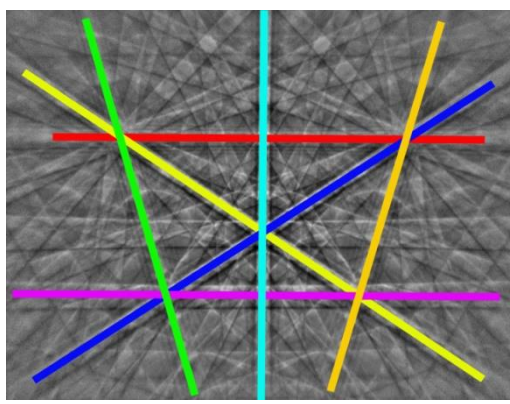
EBSD patterns acquired from a mesh of points on a sample can thus be used to produce maps of strain in that sample.



EBSP from Si



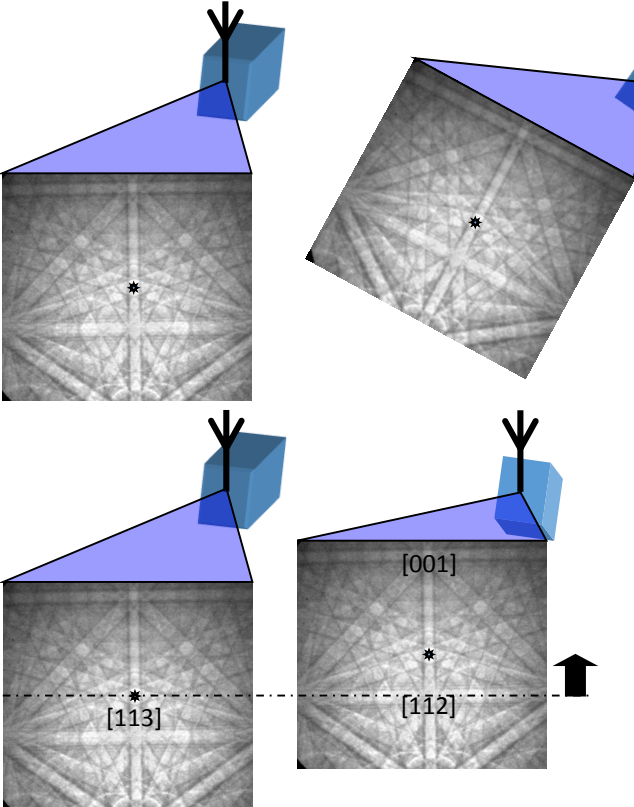
Hough transform



From: <http://www.ebsd.com/ebsd-explained/basics-of-automated-indexing>

Measuring tilt, rotation & strain with EBSD with better sensitivity

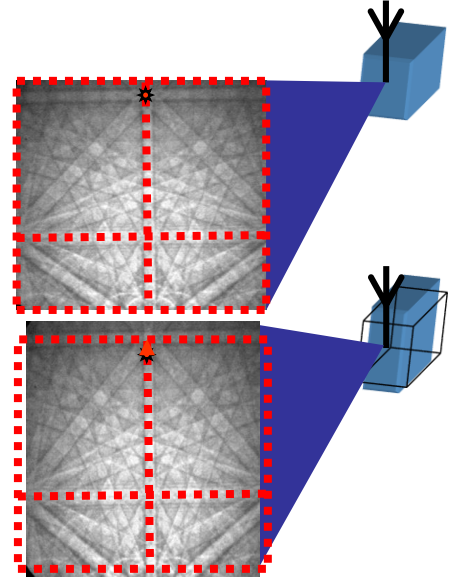
Angus Wilkinson and Arantxa Vilalta-Clemente,
Department of Materials, University of Oxford



Rotating (or twisting) a crystal rotates its EBSD pattern. This illustration shows a rotation around the * [113] direction (in silicon).

Tilting a crystal shifts its EBSD pattern. This illustration shows a tilt of $\approx 10^\circ$.

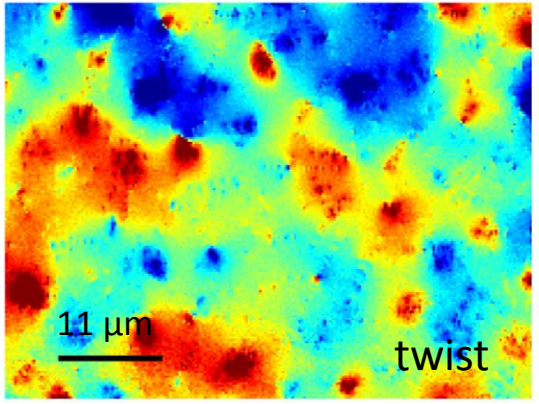
Rotations of 0.01° are measurable with cross-correlation techniques.



A distortion of a crystal will produce a distortion of the EBSD pattern.

EBSD patterns acquired from a mesh of points on a sample can thus be used to produce maps of strain in that sample.

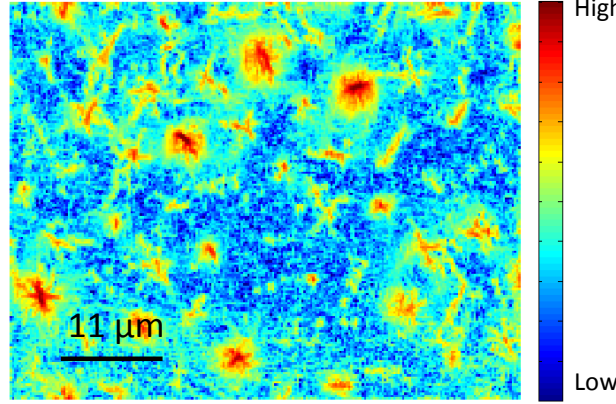
Strain changes of order 2×10^{-4} have been resolved with cross-correlation techniques.



1
0
-1
 $\times 10^{-3}$ rads

From measurement of tilt, twist and strain, geometrically necessary dislocations (GNDs) can be derived.

Measuring twist and GNDs in a GaN thin film

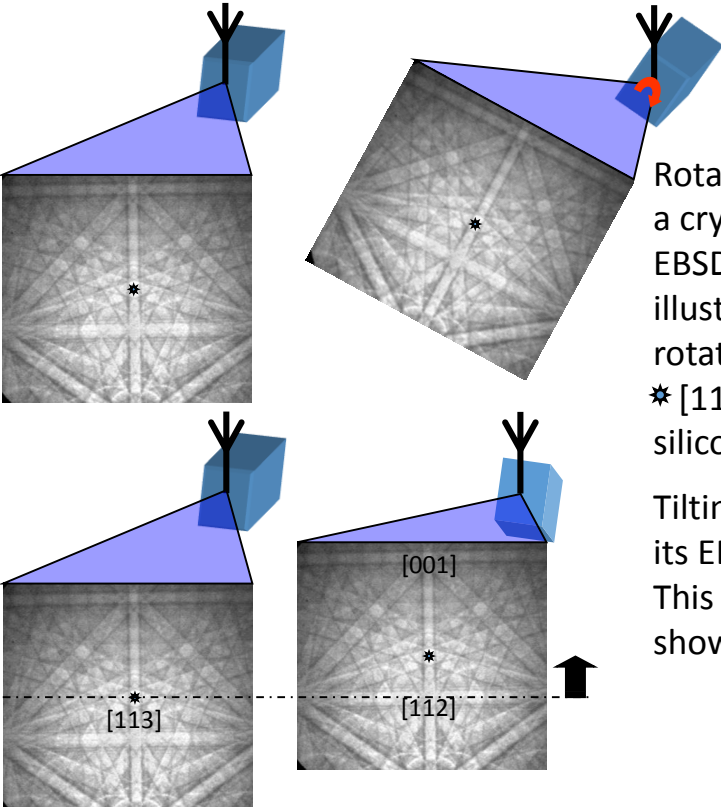


High
Low

Measuring orientation with EBSD with better sensitivity

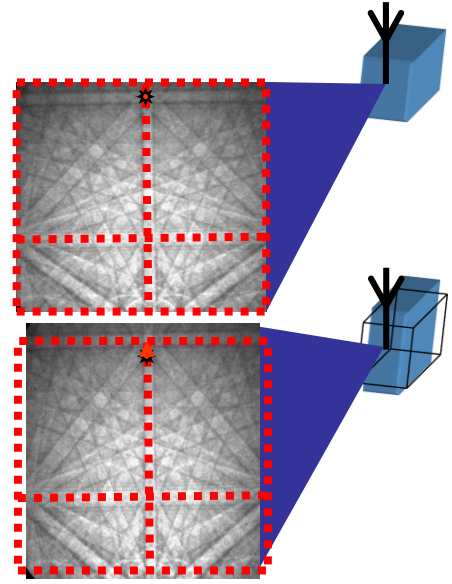
by pattern matching to dynamical simulations

– Aimo Winkelmann



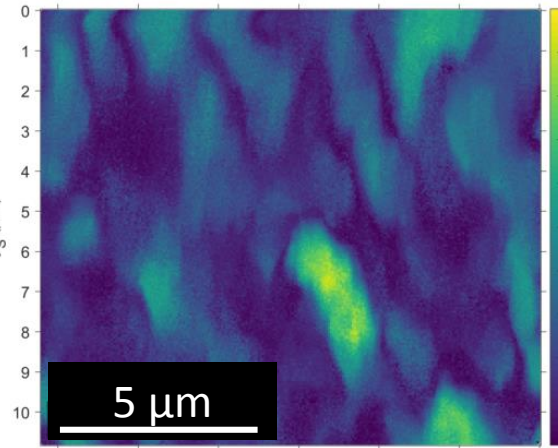
Rotating (or twisting) a crystal rotates its EBSD pattern. This illustration shows a rotation around the * [113] direction (in silicon).

Tilting a crystal shifts its EBSD pattern. This illustration shows a tilt of $\approx 10^\circ$.

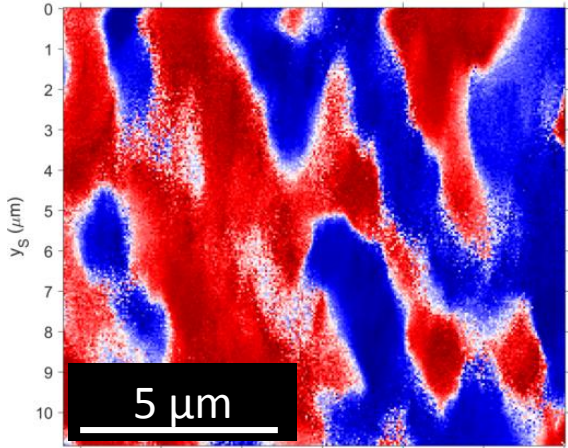


A distortion of a crystal will produce a distortion of the EBSD pattern.

EBSD patterns acquired from a mesh of points on a sample can thus be used to produce maps of strain in that sample.



0.5°
Map derived from EBSD data from c-plane AlN:
Grain reference orientation deviation (GROD)



180 degrees
Red and blue depict opposite in-plane rotations

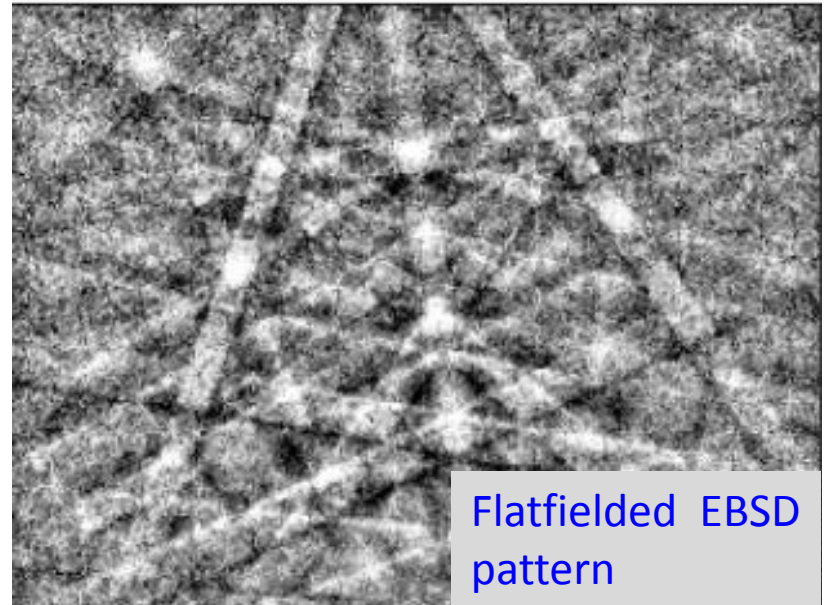
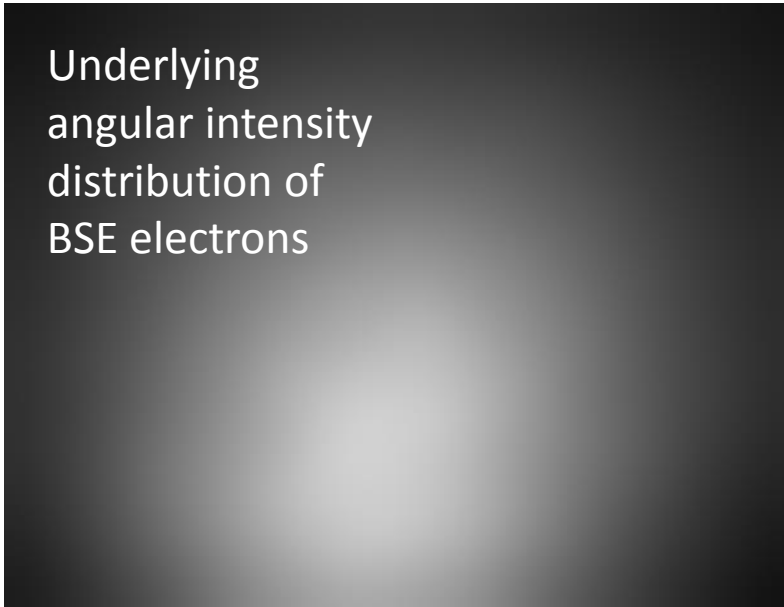
Extracting more information from EBSD patterns

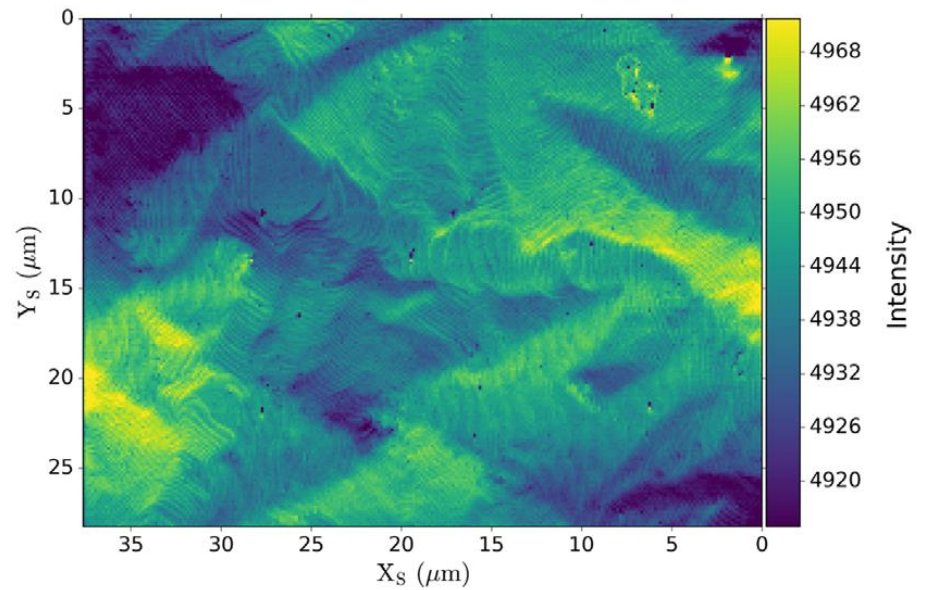
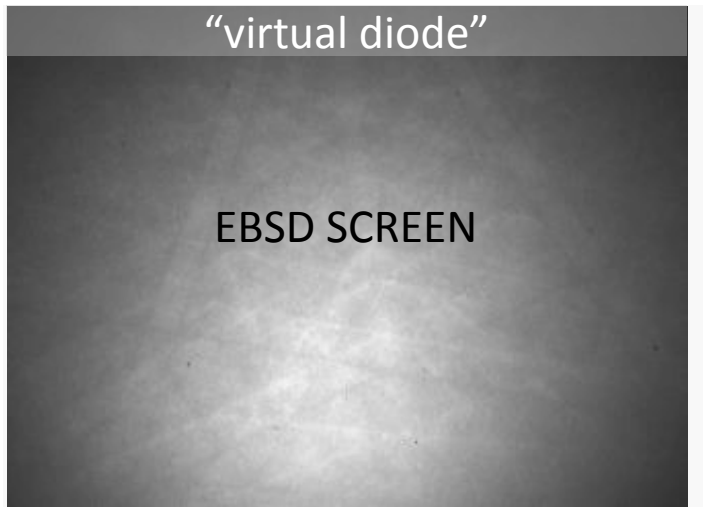
Revealing defects with EBSD

Raw EBSD
pattern

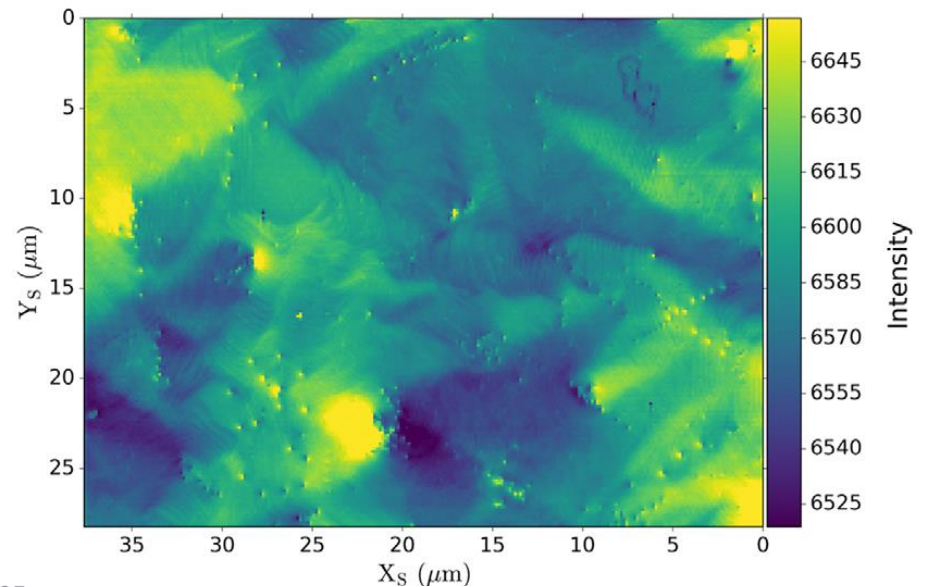
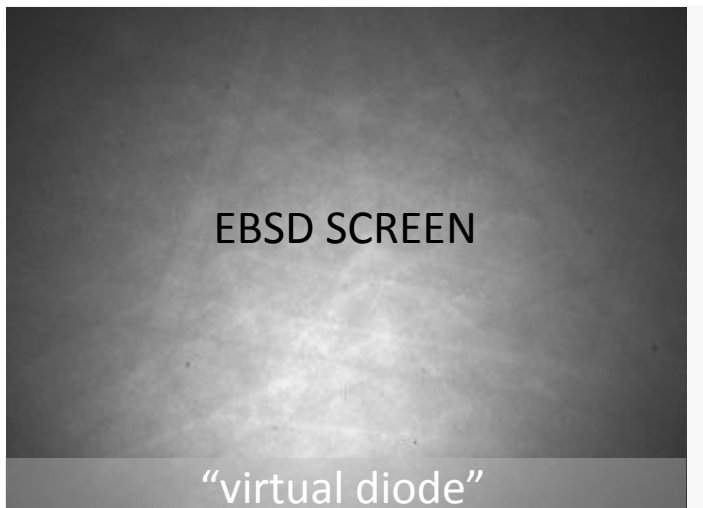


Underlying
angular intensity
distribution of
BSE electrons

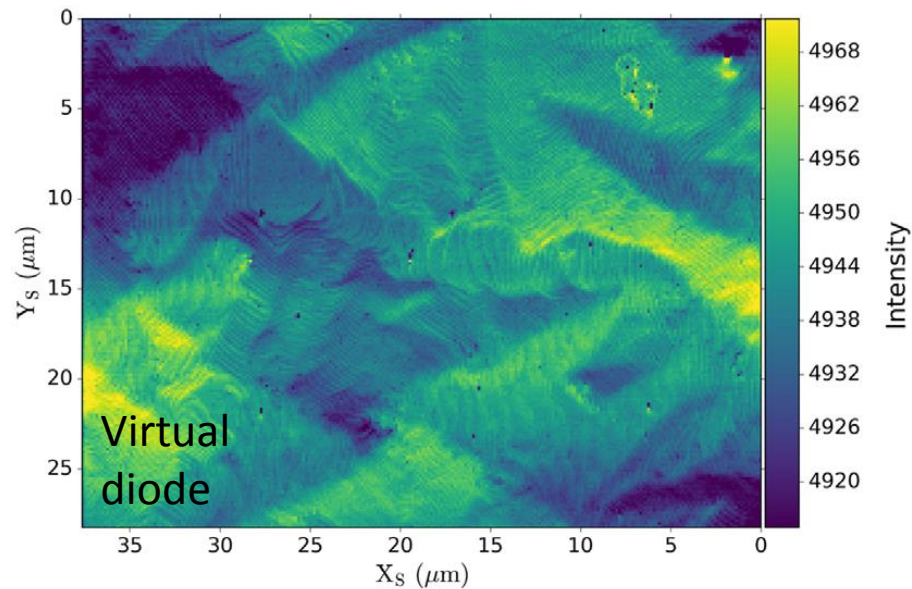




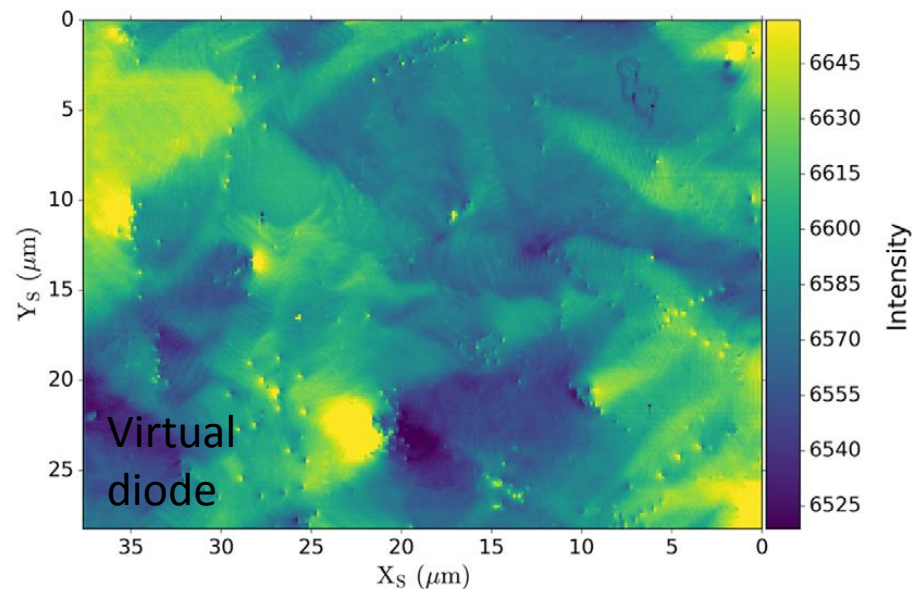
BSE signal from top 10% of **EBSD** patterns
In this case topographic contrast dominates (GaN thin film)



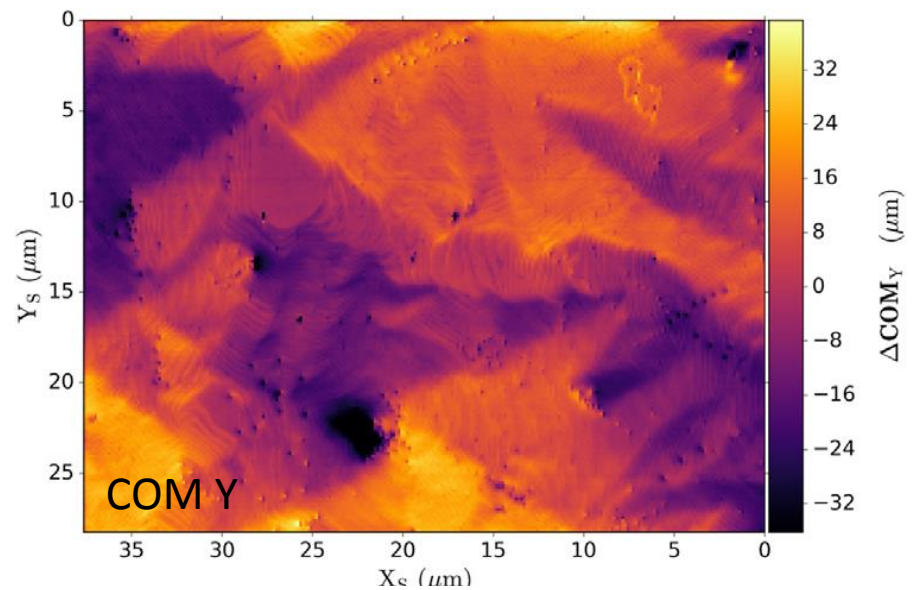
BSE signal from bottom 10% of **EBSD** patterns
In this case diffraction contrast dominates



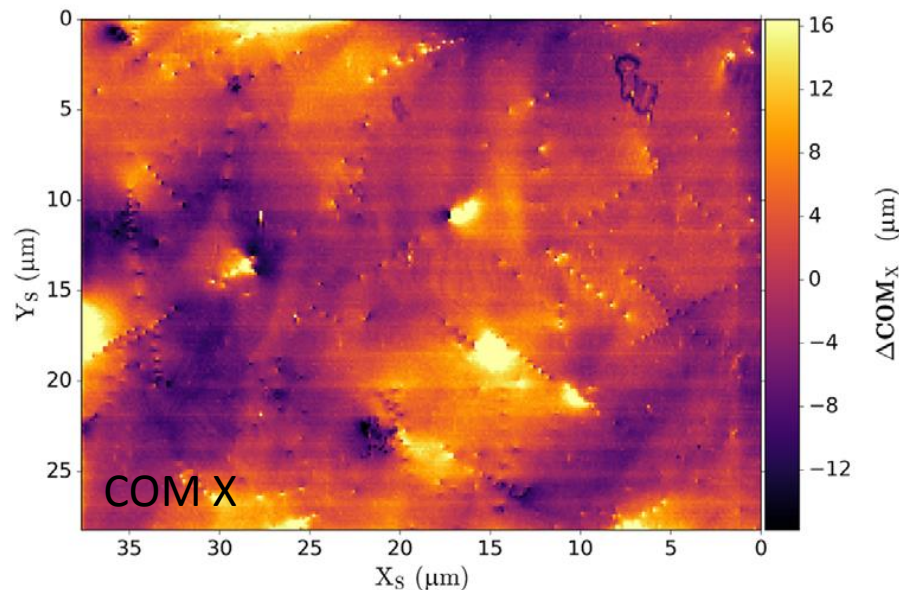
BSE signal from top 10% of **EBSD** patterns
In this case topographic contrast dominates



BSE signal from bottom 10% of **EBSD** patterns
In this case diffraction contrast dominates



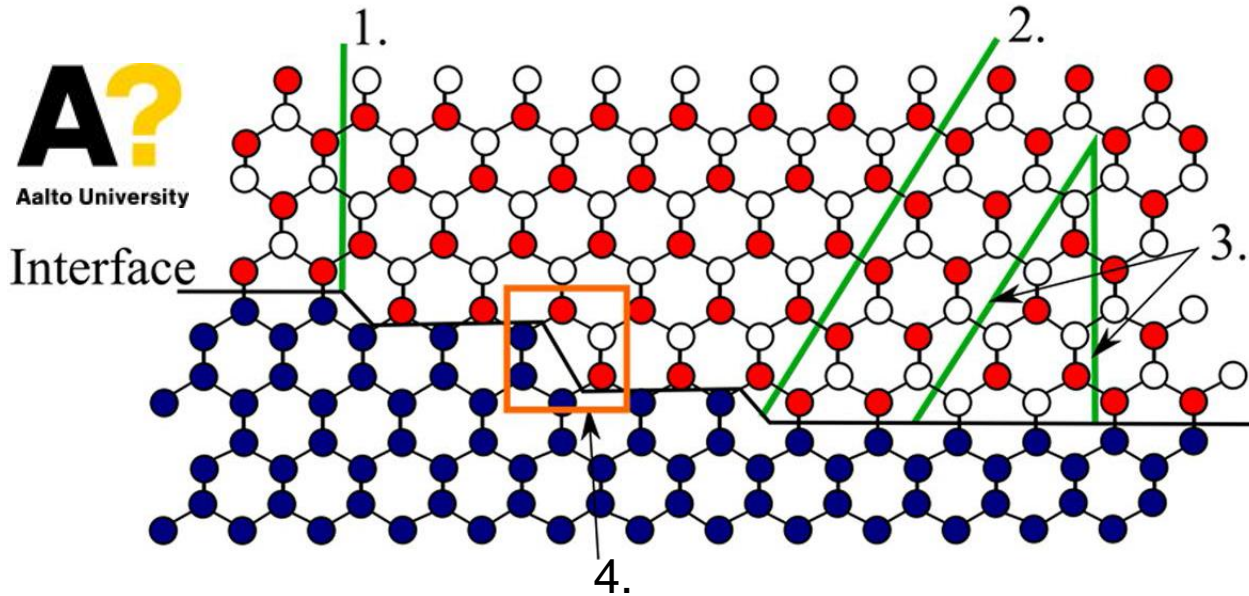
Map of y-deviation of the centre of mass of
intensity of each EBSD pattern (COM) from mean



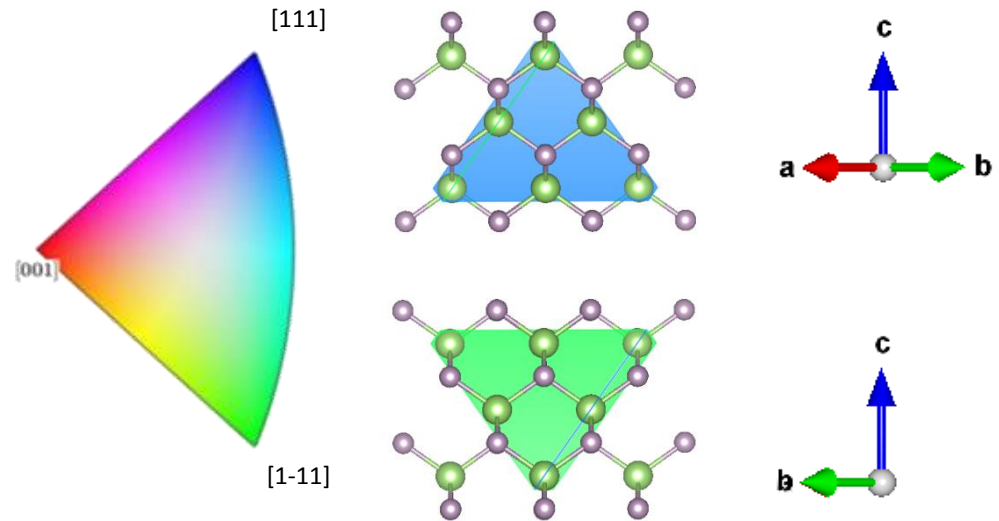
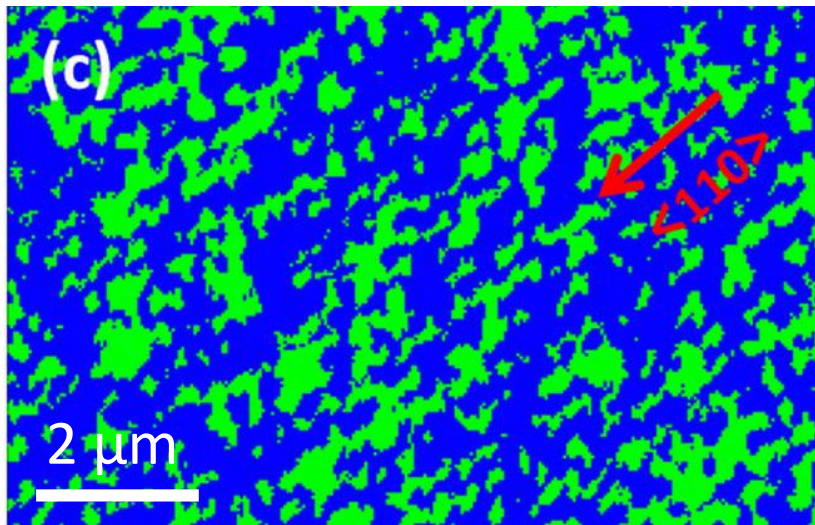
Map of x-deviation of the centre of mass of
intensity of each EBSD pattern (COM) from mean

Revealing defects with EBSD – antiphase domains (APBs) in GaP

Antiphase domains in GaP. G. Naresh-Kumar, A. Vilalta-Clemente, H. Jussila, A. Winkelmann, G. Nolze, S. Vespucci, S. Nagarajan, A. J. Wilkinson & C. Trager-Cowan, *Sci. Rep.* **7**, 10916 (2017)



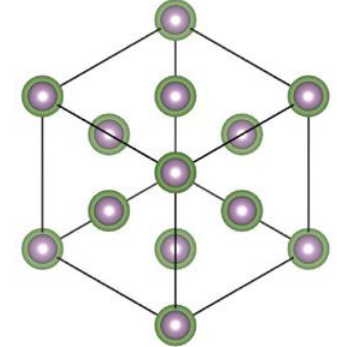
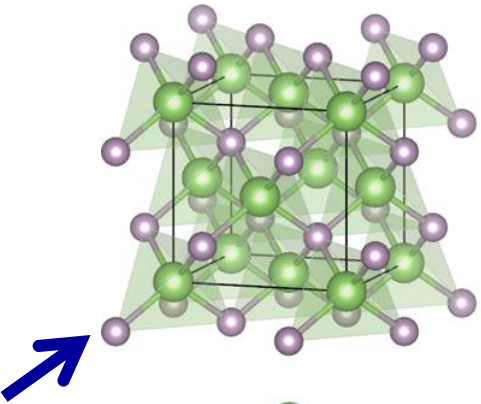
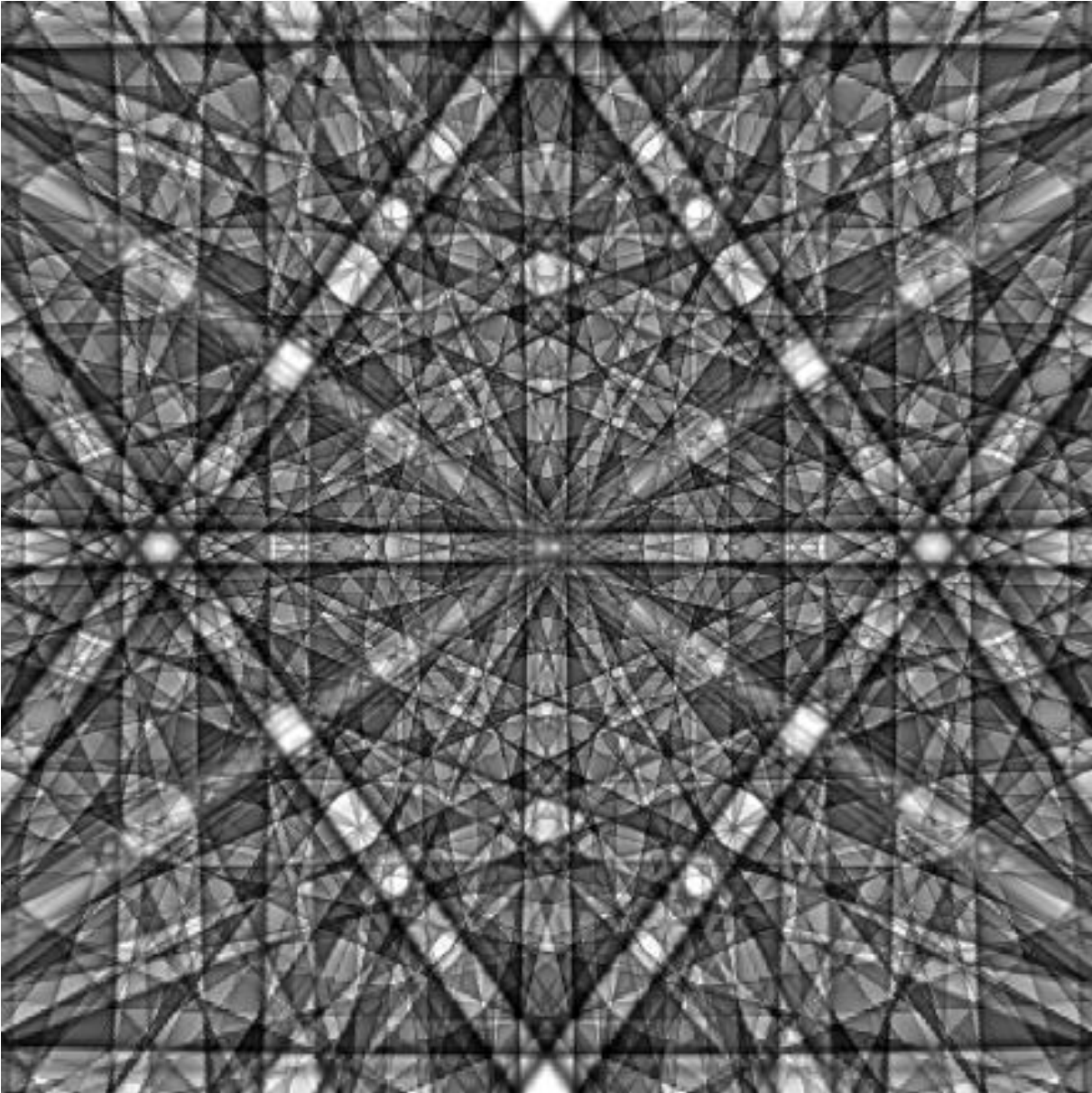
- Silicon atom
 - Phosphorus atom
 - Gallium atom
1. APBs parallel to (110)
 2. APBs along the {111}Si
 3. annihilation of APBs along (111) and (110) and
 4. annihilation of APBs due to diatomic steps.



EBSD inverse pole figure (IPF) map revealing the APDs produced from cross-correlation with dynamical simulations

K. Momma and F. Izumi, "VESTA 3 for three-dimensional visualization of crystal, volumetric and morphology data," *J. Appl. Crystallogr.*, **44**, 1272-1276 (2011) & <https://github.com/cryos/avogadro/blob/master/crystals/phosphides/GaP.cif>

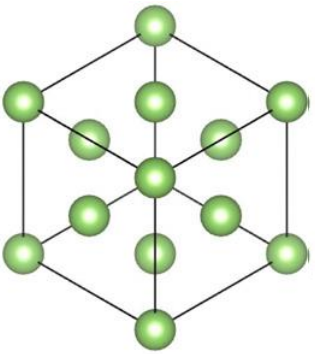
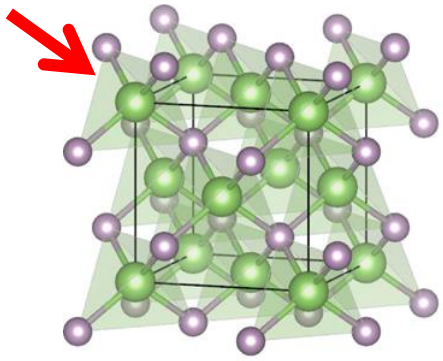
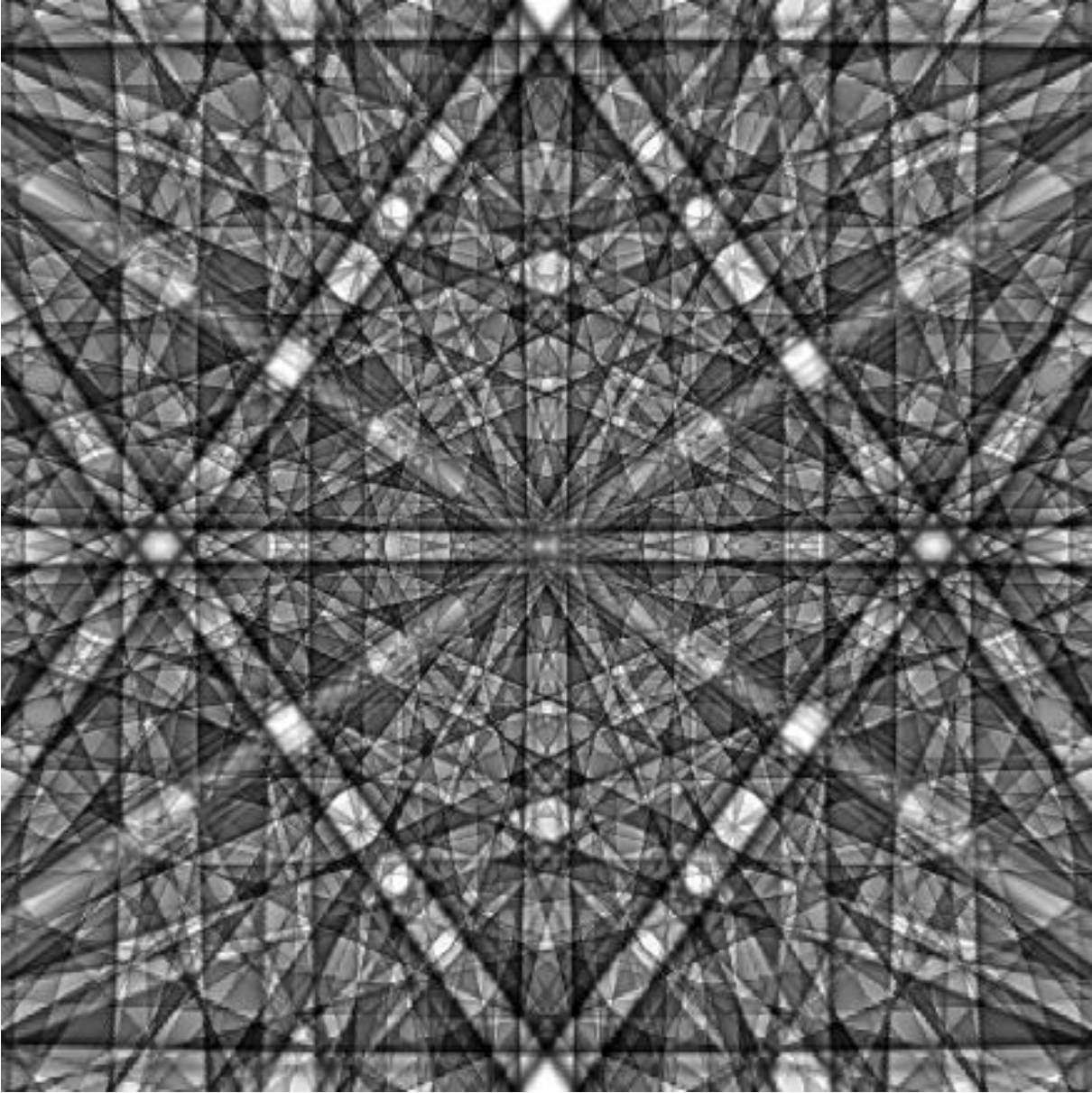
APBs in GaP – revealed through non-centrosymmetry



— (1-11)
— (111)

Dynamical simulation of EBSD pattern from GaP (15 keV)

APBs in GaP – revealed through non-centrosymmetry

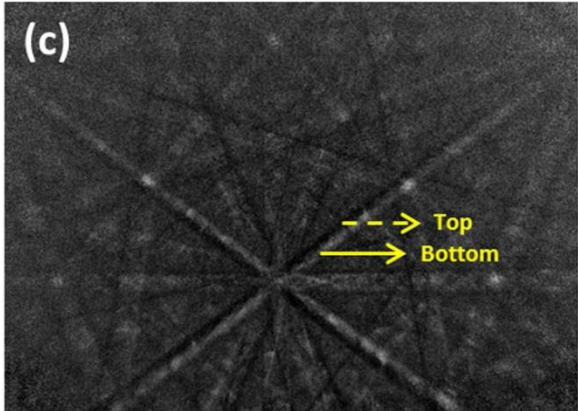
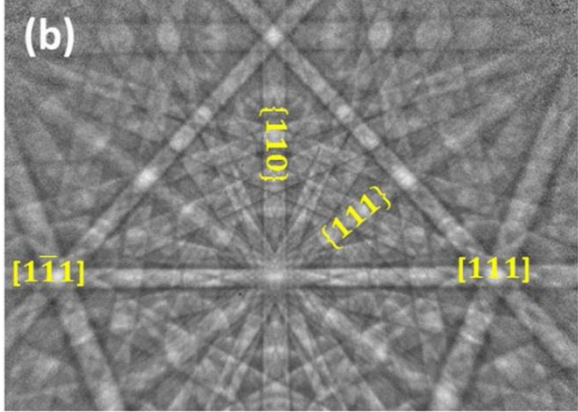
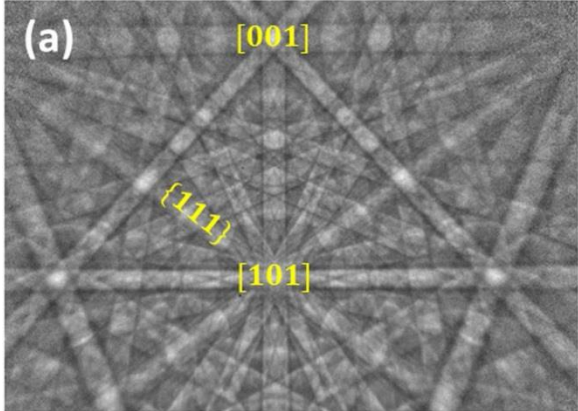


— (1-11)
— (111)

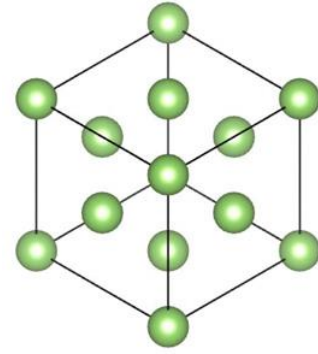
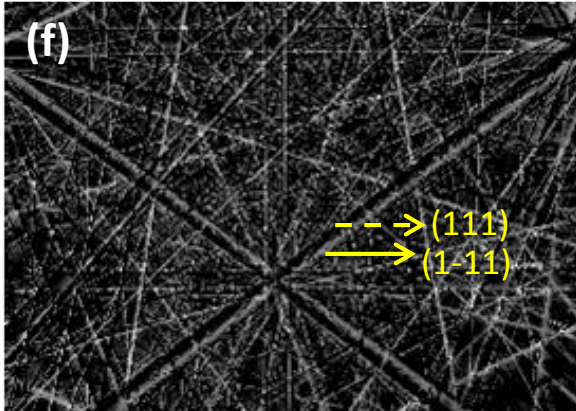
Dynamical simulation of EBSD pattern from GaP (15 keV)

APBs in GaP – revealed through non-centrosymmetry

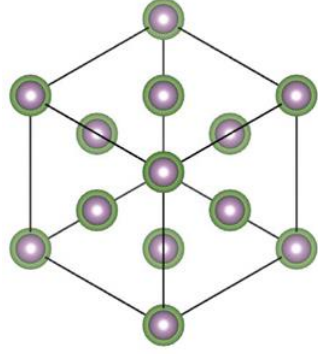
Experiment



Difference between experimental patterns



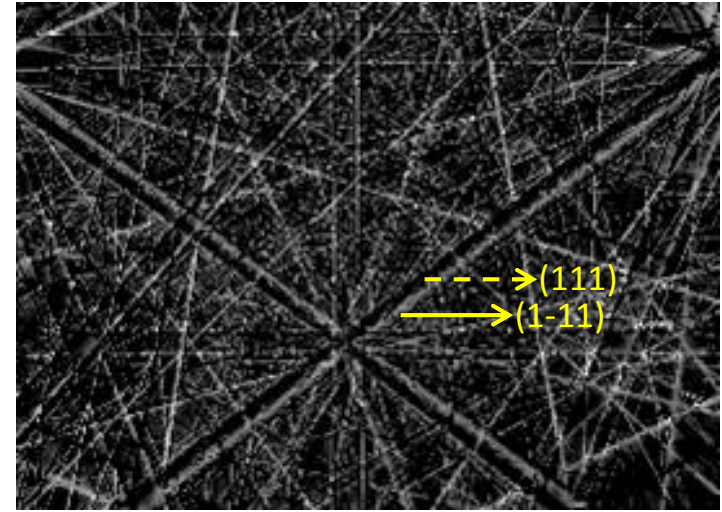
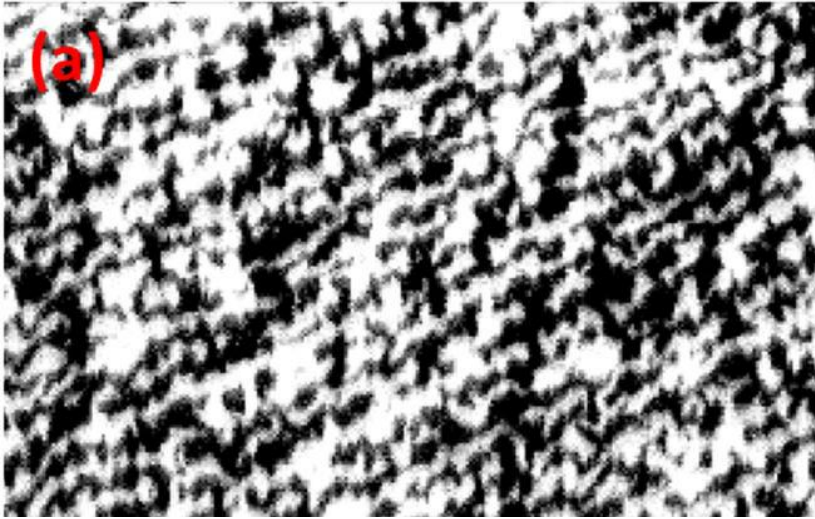
Theory



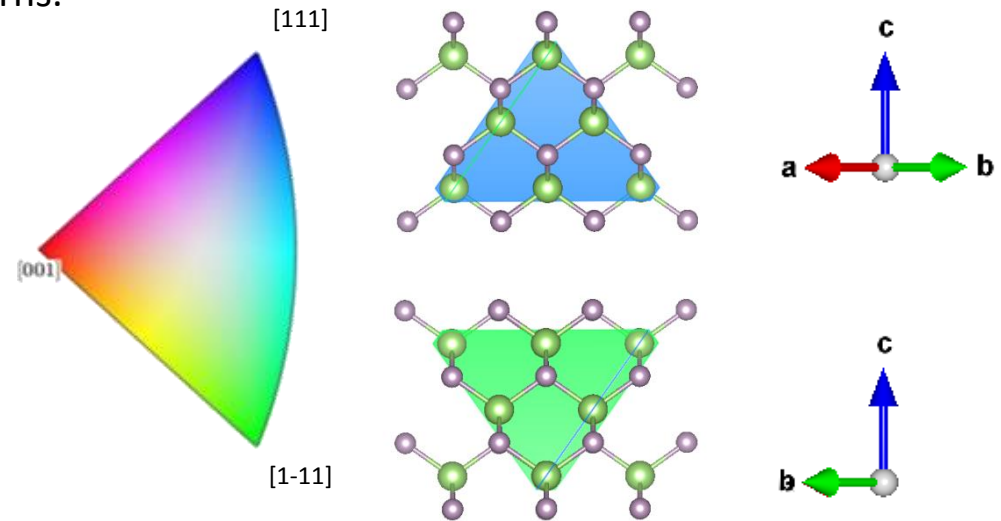
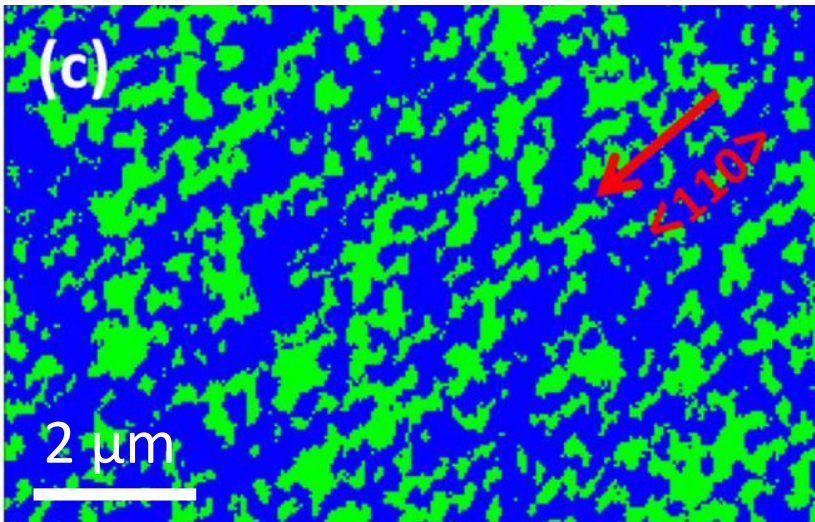
Difference between theoretical patterns

Revealing defects with EBSD – antiphase domains (APBs) in GaP

Antiphase domains in GaP. G. Naresh-Kumar, A. Vilalta-Clemente, H. Jussila, A. Winkelmann, G. Nolze, S. Vespucci, S. Nagarajan, A. J. Wilkinson & C. Trager-Cowan, *Sci. Rep.* **7**, 10916 (2017)



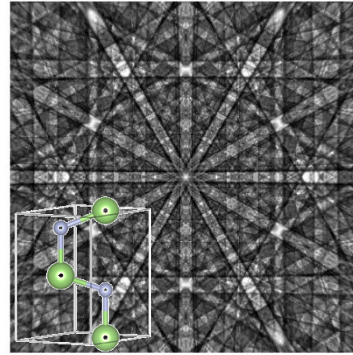
Region of interest asymmetry imaging from the $\{111\}$ bands produced from background corrected EBSD patterns.



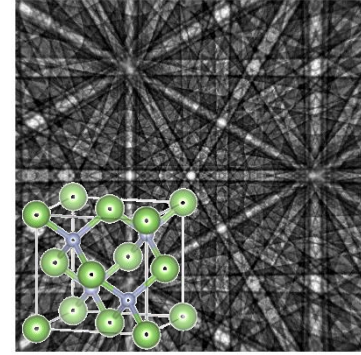
EBSD inverse pole figure (IPF) map revealing the APDs produced from cross-correlation with dynamical simulations

To summarise what we can measure:

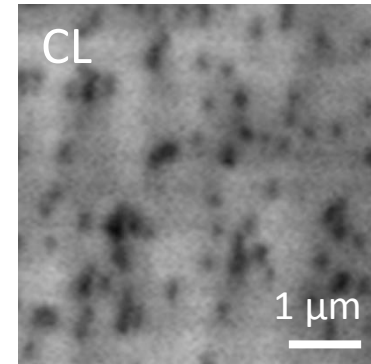
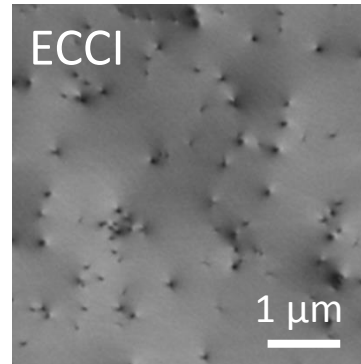
- Crystal structure
- Crystal orientation
- Misorientation
- Grain size
- Grain boundaries
- Strain
- Structural defects, in particular extended defects
 - dislocations
 - stacking faults



EBSP Wurtzite GaN



EBSP Zincblende GaN

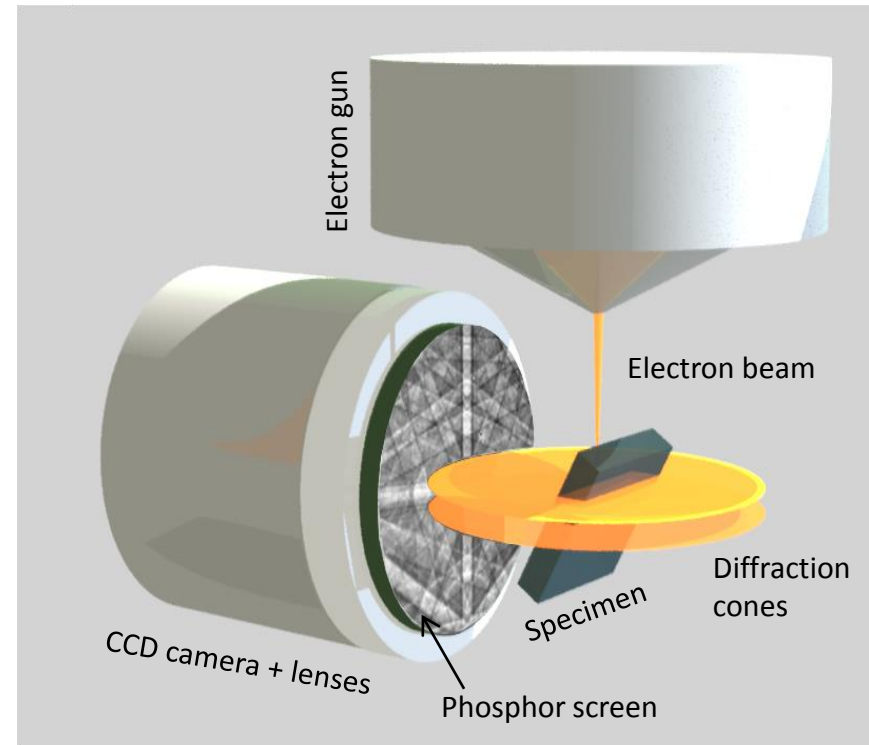


In particular if EBSD is used with electron channeling contrast imaging (ECCI)

The influence of the structural properties on the light emission properties of materials can be determined if EBSD and ECCI are used together with cathodoluminescence (CL)

Limitations of conventional EBSD systems

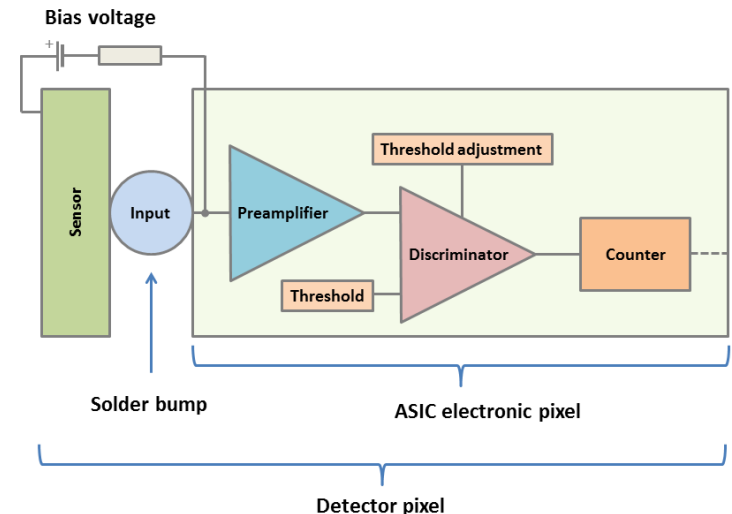
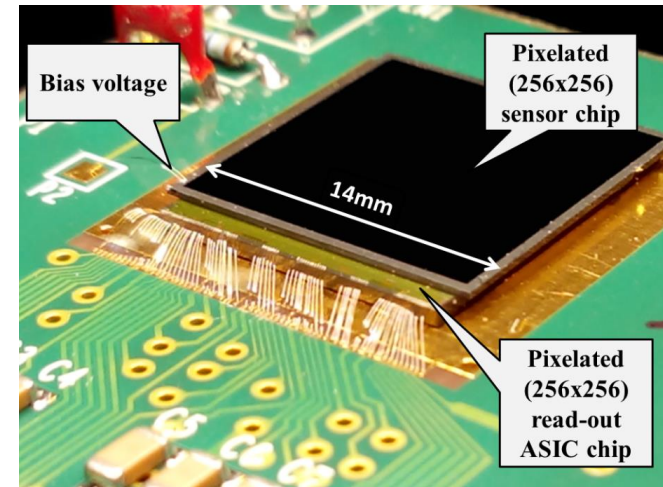
- Inefficient conversion of electrons to light, and light back to electrons
- Intrinsic light scattering and optical interference within the phosphor
→ intrinsic loss of spatial resolution
- Intrinsic noise of the CCD camera
→ reduced signal to noise ratio
- Distortion of the pattern due to the optics
- Inability to select electrons having a specific energy range



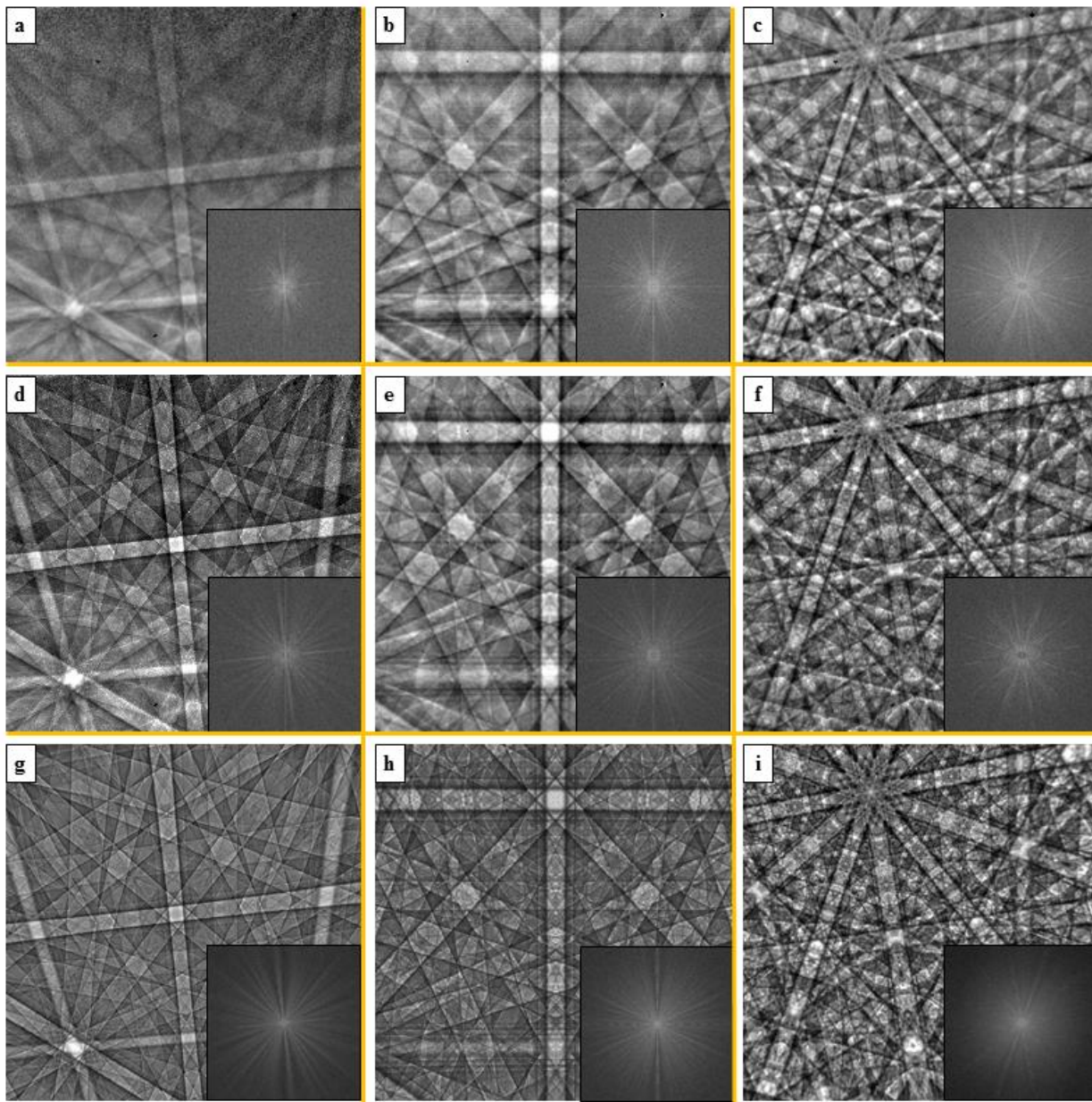
Advantages of direct electron detection, with hybrid pixel detectors, for EBSD pattern acquisition

- Sensor separated from the electronics:
 - Radiation hardness
- Direct electron imaging:
 - Can use lower electron beam currents and voltages – lower dose, exciting for characterisation of materials which damage under electron beam irradiation
 - Improvement in lateral and depth resolution
 - no need for distorting optics
- Energy discrimination:
 - Work in noise-free conditions
 - Energy filtered EBSD pattern
 - Improved contrast and sharpness of electron backscatter patterns (EBSPs)
 - Increase in detail in EBSPs
 - Improvement in lateral and depth resolution
- Compact size

Timepix detector



Energy filtering direct electron detectors and dynamical simulations for EBSD



Diamond

Silicon

GaN

Low filtered

High filtered

Simulations

Experimental and simulated EBSDs from diamond (a),(d) (g), Si (b), (e), (h) & GaN (c), (f), (i) for an incident beam energy of 20 keV, and a probe current of ≈ 10 nA

(a), (b) and (c) were acquired with a high pass energy filter of 4.6 keV

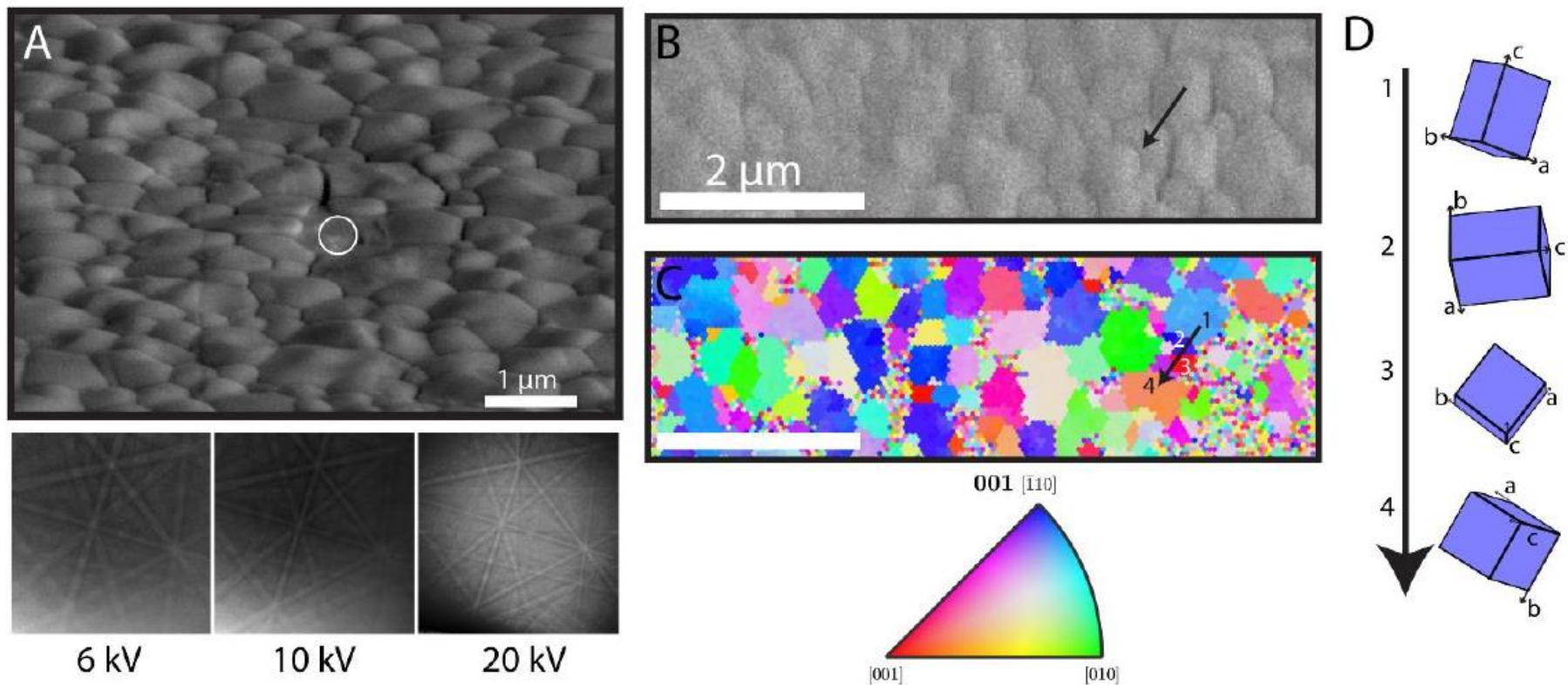
(d), (e) and (f) were acquired with a high pass energy filter of 19.4 keV

(g), (h) and (i) are simulations
The insets are 2D fast Fourier transforms of each image.



Digital direct electron imaging of energy filtered electron backscatter diffraction patterns, S. Vespucci et al, Phys. Rev. B. **92** 205301 (2015)

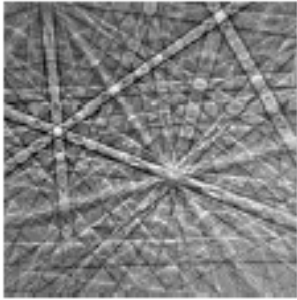
Example application – EBSD of Halide Perovskites



Morphology and local crystal orientation measurements of $\text{CH}_3\text{NH}_3\text{PbI}_3$ thin films. (A) SEM image of $\text{CH}_3\text{NH}_3\text{PbI}_3$ thin film tilted at 45° with representative sharp Kikuchi diffraction lines of a measurement point inside a grain (circled) collected in EBSD geometry at 6 kV, 10 kV and 20 kV accelerating voltage. (B) SEM image and (C) Inverse Pole Figure (IPF) map generated from EBSD of a representative $\text{CH}_3\text{NH}_3\text{PbI}_3$ film with IPF color key. The 001(in bold) in the IPF color key indicates that the IPF map plotted is along the sample z-direction. (D) Depiction of changes in local crystal orientation along the black arrow in (B) and (C) as viewed normal to the sample. EBSD conditions - 100 pA at 6 kV accelerating voltage with a pixel integration time of 100 ms.

From: Jariwala S, Sun H, Adhyaksa GW, Lof A, Garnett EC, Ginger DS. Imaging Grain Structure in Halide Perovskites: Local Crystal Misorientation Influences Non-Radiative Recombination. arXiv preprint arXiv:1903.11033. 2019 Mar 26.

Commercial applications



Direct Electron Detection with Clarity™ - Viewing EBSD Patterns in a New Light

Summary

The removal of the optical pathway in the detection of electrons and direct counting of the diffracted electrons that contribute to the Electron Backscatter Diffraction (EBSD) patterns allow for more detailed analysis of pattern generation. In this presentation, the differences between traditional EBSD detectors and direct detection are highlighted and new possibilities are explored.

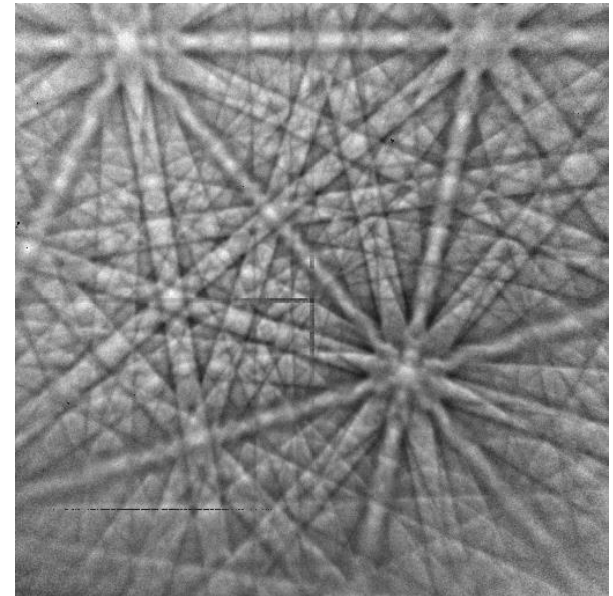
Speakers



Dr. René de Kloe
Applications Specialist
EDAX Inc.

Webinar broadcast on 21/09/2016

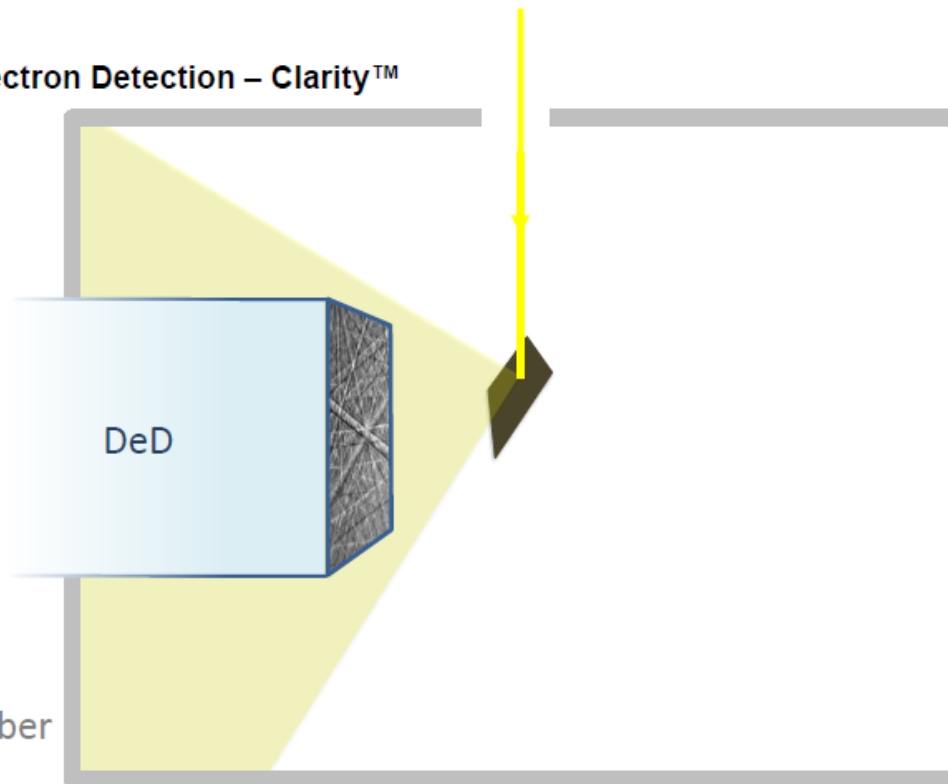
The EDAX Clarity™ detector is based on 2 × 2 Timepix chips
(QUAD)



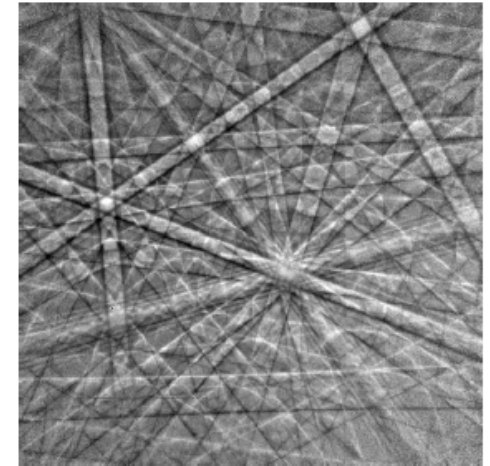
Slide from “Direct Electron Detection with Clarity™ - Viewing EBSD Patterns in a New Light” presentation

Back to the future

- EDAX – 2019
 - Direct electron Detection – Clarity™
 - CMOS
 - Digital



Vespucci, S., Winkelmann, A., Naresh-Kumar, G., Mingard, K.P., Maneuski, D., Edwards, P.R., Day, A.P., O'Shea, V. and Trager-Cowan, C., 2015. Digital direct electron imaging of energy-filtered electron backscatter diffraction patterns. *Physical Review B*, 92(20), p.205301.



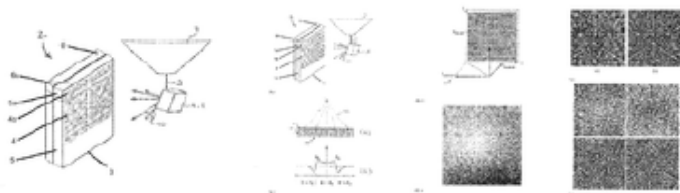
Patent

Method and system for determining the position of a radiation source

Abstract

The present invention refers to a method for determining a position of a divergent radiation source (1), comprising irradiating a pixel detector (2) with a predetermined intensity distribution of radiation with wavelength λ originated from the radiation source (1), wherein the pixel detector (2) comprises a plurality of pixels with pixel coordinates (x_i, y_i, z_i) ; Detecting, for each of the plurality of pixels, an intensity of the incident radiation (10); Determining, for each of the plurality of pixels, an incidence direction of the incident radiation using information on an orientation of an internal periodic structure at the pixel and the predetermined intensity distribution, wavelength λ and the detected intensity; and Determining the position (x_p, y_p, z_p) of the radiation source (1) using the pixel coordinates (x_i, y_i, z_i) and the incidence direction for each of the plurality of pixels. The invention further refers to a system, a computer-related product and a sample (8) for performing such method and to the use of a pixel detector (2) for determining a position of a divergent radiation source (1).

Images (4)



Classifications

■ [G01B15/00](#) Measuring arrangements characterised by the use of wave or particle radiation

[View 3 more classifications](#)

US10234282B2

United States

[Download PDF](#)

[Find Prior Art](#)

[Similar](#)

Inventor: [Aimo WINKELMANN](#), [Stefano VESPUCCI](#)

Current Assignee: [Brunker Nano GmbH](#), [Bruker Nano GmbH](#), [University of Strathclyde](#)

Worldwide applications

2016 [EP](#) 2017 [US](#) [JP](#)

Application US15/643,344 events ⓘ

2016-07-07 [Priority to EP16178468](#)

2017-07-06 [Application filed by Brunker Nano GmbH, University of Strathclyde](#)

2018-01-11 [Publication of US20180010909A1](#)

2019-03-19 [Publication of US10234282B2](#)

2019-03-19 [Application granted](#)

2019-11-23 [Application status is Active](#)

2037-07-06 [Anticipated expiration](#)

[Show all events](#) ▾

Info: [Patent citations \(3\)](#), [Non-patent citations \(11\)](#), [Legal events](#), [Similar documents](#), [Priority and Related Applications](#)

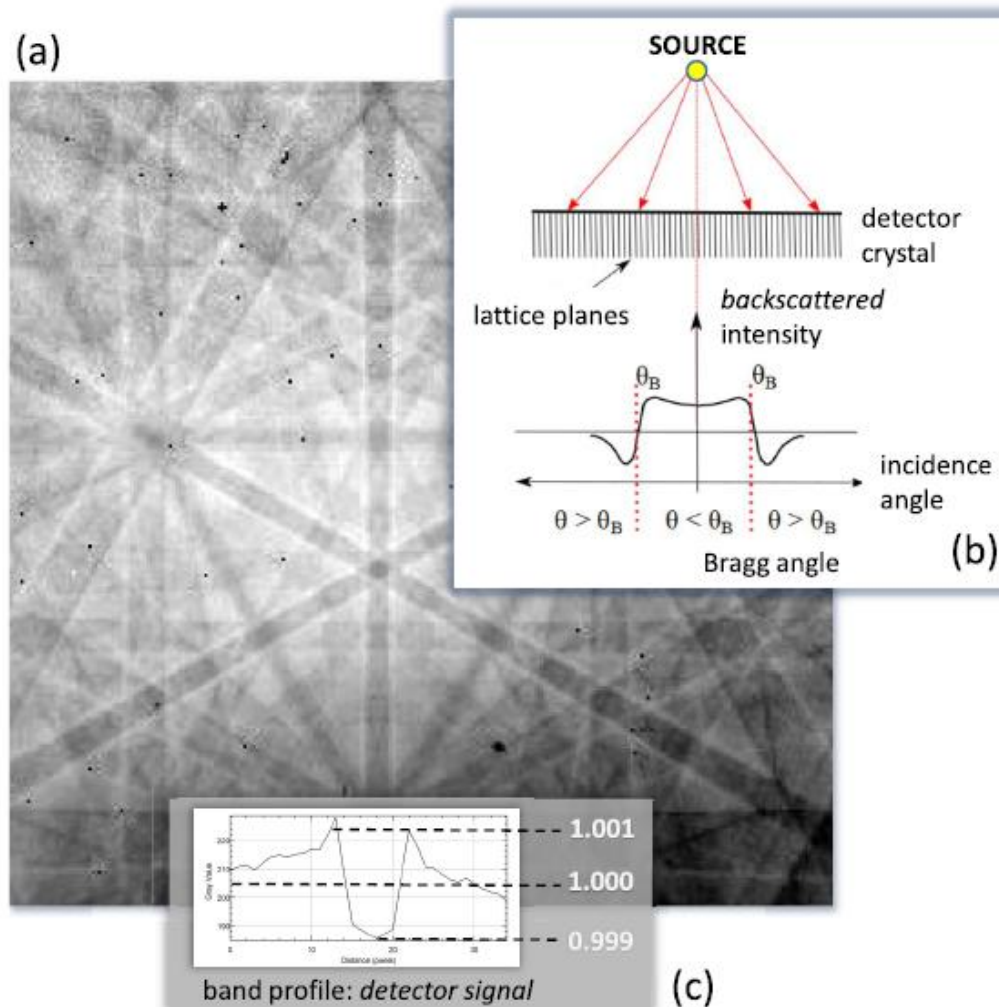


FIG. 2. Measured signal on the Timepix detector. Pixel(angle)-dependent electron absorption measured on the TimePix detector. Electron channeling effect of electron waves incident on a single-crystalline detector.

From: Vespucci S, Naresh-Kumar G, Trager-Cowan C, Mingard KP, Maneuski D, O'Shea V, Winkelmann A. "Diffractive triangulation of radiative point sources." *Applied Physics Letters*. 2017 Mar 20;110(12):124103.

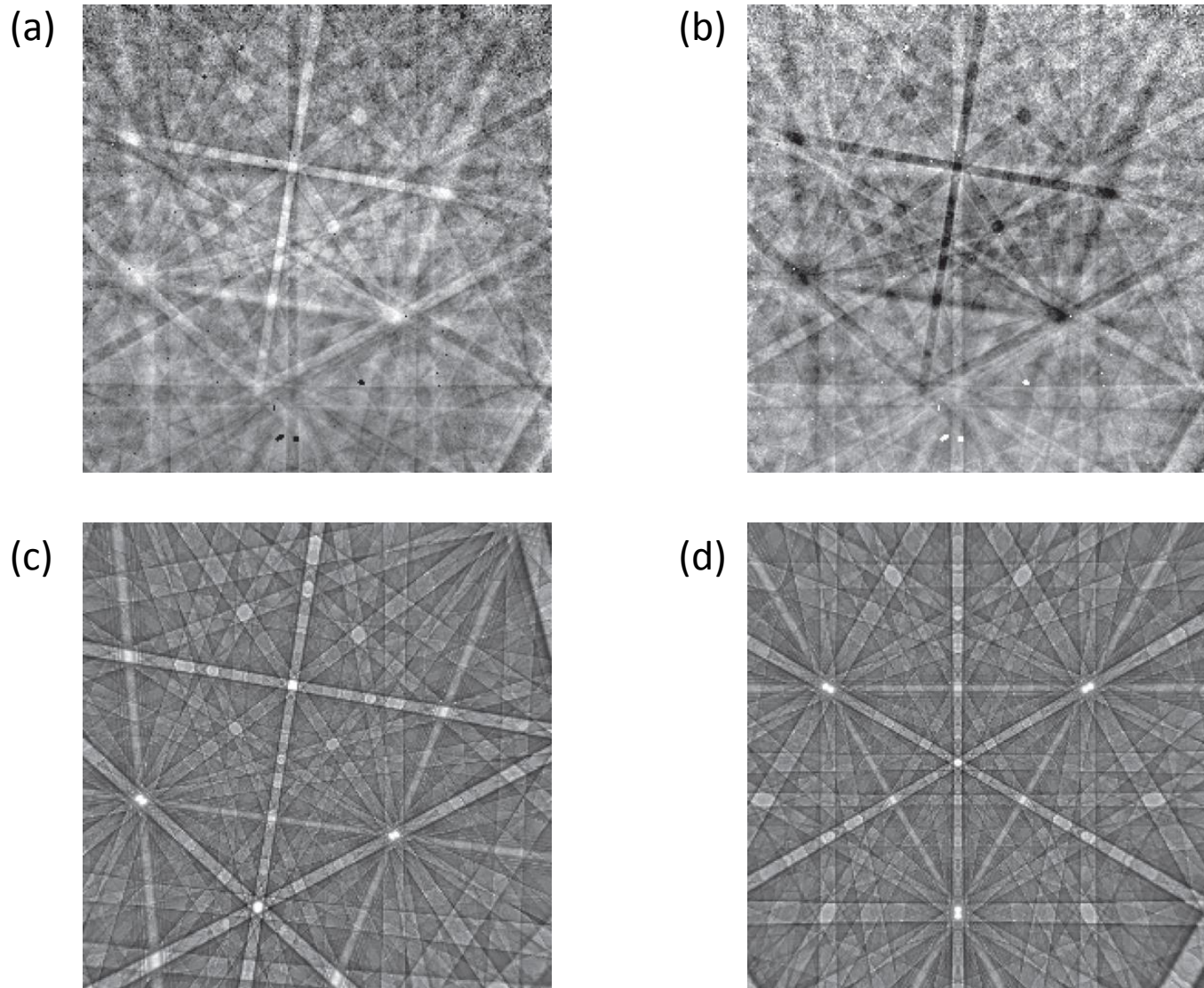


FIG. 4. Backscattered electron diffraction measurement at 25 keV obtained from a film of 10 nm HfO_2 on Si (001) using a Timepix detector. (a) Measurement containing simultaneously a detector diffraction pattern (DDP, dark bands) together with a backscatter Kikuchi pattern (BKP, light bands) of the silicon sample. (b) Negative of the left pattern (d) Best-fit simulation of the pattern structure corresponding to the DDP. This gives the projection point (x_P , y_P , and z_P). (c) Best-fit simulation of the BKP corresponding to the sample orientation of ($\phi_1 = 179.95$; $\Phi = 19.93$; $\phi_2 = 215.59$), assuming the projection center determined via (d).

Requirements for next generation direct electron detectors for EBSD

- Existing chips already offer the benefits of operating at lower current and voltages, can we do better?
- Can energy filtering be improved – towards spectroscopy?
- Can we go to a 40 mm × 40 mm device with 2k × 2k pixels (20 μm × 20 μm pixel size)?
- Can we acquire images faster? Existing EBSD systems can go up to 4500 patterns per second.